

A Silver DNAzyme

Runjhun Saran and Juewen Liu*

Department of Chemistry, Waterloo Institute for Nanotechnology,
University of Waterloo

Waterloo, Ontario, Canada, N2L 3G1.

Phone: 519-888-4567, extension 38919

Email: liujw@uwaterloo.ca

Abstract

Silver is a very common heavy metal, and its detection is of significant analytical importance. DNazymes are DNA-based catalysts; they typically recruit divalent and trivalent metal ions for catalysis. Herein, we report a silver-specific RNA-cleaving DNzyme named Ag10c obtained after six rounds of in vitro selection. Ag10c displays a catalytic rate of 0.41 min^{-1} with $10 \text{ }\mu\text{M Ag}^+$ at pH 7.5 with 200 mM NaNO_3 , while its activity is completely inhibited with the same concentration of NaCl. Ag10c is highly specific for Ag^+ among all the tested metals. A catalytic beacon biosensor is designed by labeling a fluorophore and a quencher on the DNzyme. Fluorescence enhancement is observed in the presence of Ag^+ with a detection limit of 24.9 nM Ag^+ . The sensor shows a similar analytical performance in Lake Huron water. This is the first monovalent transition metal dependent RNA-cleaving DNzyme. Apart from its biosensor application, this study strengthens the idea of exploring beyond the traditional understanding of multivalent ion dependent DNzyme catalysis.

Introduction

Metallic silver, its alloys and compounds have been used in jewellery, solar cells, antimicrobial agents, dental amalgams, photography, electronic components, glass coatings and catalysis, among other applications.¹ Such widespread usage has led to environmental contamination. Silver is a heavy metal and poses a health threat as it tends to bioaccumulate, causing damages to the skin, eyes, liver, kidneys and intestinal tracts.² While silver can be measured by instrumentation methods such as ICP-MS, it is also important to develop biosensors for on-site detection, which may also help recover this valuable metal.^{3,4}

Over the past two decades, DNA has emerged as a highly versatile platform for metal sensing based on either metal/nucleobase binding interactions or metal-assisted DNAzyme catalysis.⁵⁻¹⁰ RNA-cleaving DNAzymes are particularly interesting since they can achieve extremely high metal sensitivity and are versatile in biosensor design.^{11, 12} DNAzymes are DNA-based catalysts isolated using in vitro selection.¹³ They often recruit divalent metals for catalysis, and in vitro selections can be intentionally performed to evolve DNAzymes that work only in the presence of specific metals.¹⁴ Many divalent metals including Pb^{2+} ,¹⁵ Zn^{2+} ,¹⁶ Cu^{2+} ,^{17, 18} UO_2^{2+} ,¹⁹ Cd^{2+} ,²⁰ and Hg^{2+} have been detected using DNAzymes.²¹ Recently, important advancements have been made on trivalent metals as well; we isolated and a few lanthanide-dependent DNAzymes.^{12,}

22-24

The perception of multivalent metals requirement was relaxed by the recent discovery of DNAzymes that use only monovalent Na^+ .²⁵⁻²⁷ For example, the Lu group reported a DNAzyme with a rate of $\sim 0.1 \text{ min}^{-1}$ using Na^+ as the sole metal.²⁷ To reach such a high rate, however, 400 mM Na^+ is needed. The same Na^+ binding motif was also identified in another lanthanide-dependent DNAzyme.^{24, 28, 29} We isolated a Na^+ -specific DNAzyme named EtNa, also requiring

high mM Na⁺ in water but low mM Na⁺ in ethanol.³⁰ It remains unclear whether it is possible to obtain DNAzymes that can work with nanomolar transition metals. If existing, these DNAzymes will be not only analytically useful, but can answer fundamental questions in bioinorganic DNA chemistry.

The most studied interaction between DNA and silver is the specific binding between the cytosine base and Ag⁺.^{31, 32} This interaction was used to develop Ag⁺ biosensors,³³⁻³⁵ and for making fluorescent silver nanoclusters.^{36, 37} While DNAzymes have also been used for Ag⁺ detection,³⁵ these sensors still rely on the capturing of Ag⁺ by cysteine pairs, and Ag⁺ does not participate in catalysis. Herein, we report the first Ag⁺-specific RNA-cleaving DNAzyme named Ag10c, and a highly sensitive and selective biosensor using this DNAzyme.

Materials and Methods

Chemicals. The *in vitro* selection and sensing related DNA samples were from Integrated DNA Technologies (Coralville, IA). The rest of the DNAs were from Eurofins (Huntsville, AL). AgNO₃ and other metal salts were from Sigma–Aldrich at the highest purity available. Sodium acetate, 2-(*N*-morpholino) ethanesulfonic acid (MES), 3-(*N*-morpholino) propanesulfonic acid (MOPS), ethylenediaminetetraacetic acid (EDTA) disodium salt dihydrate, sodium chloride and ammonium acetate were from Mandel Scientific Inc. (Guelph, Ontario, Canada). Sso Fast EvaGreen supermix was from Bio-Rad. T4-DNA ligase, deoxynucleotide (dNTP) mix, Taq DNA polymerase with ThermoPol buffer and low molecular weight DNA ladder were from New England Biolabs.

In vitro selection. The method of *in vitro* selection was derived from our previous report with some minor modifications.²⁴ In brief, the initial library was obtained by ligating Lib-FAM-N50 and Lib-rA (see Table S1 for DNA sequences). For each subsequent round, the library was

produced by PCR. For each cleavage step, a freshly prepared AgNO_3 solution was added to the DNA library in buffer A (50 mM MES, pH 6.0, 25 mM NaNO_3) with 60 min incubation (final 10 μM Ag^+). After incubation, the library was mixed with 8 M urea and purified by 10% dPAGE (denaturing polyacrylamide gel electrophoresis). The position corresponding to the cleavage product was excised from the gel, the DNA was extracted by crushing and soaking the gel, and the sample was further desalted with a Sep-Pak C18 column (Waters). After drying in an Eppendorf Vacufuge at 30 °C overnight, the dried DNA was re-suspended in 60 μL of 5 mM HEPES buffer (pH 7.5). A small fraction of this DNA was amplified by two rounds of PCR (PCR1 and PCR2) using previously described thermocycling conditions.²⁴

Deep sequencing. To prepare sample for deep sequencing, the round 6 library was subjected to PCR1 as explained above. The full-length library generated from this step was subjected to another PCR reaction so that the Illumina sequencing technology can be used. The forward primer (P701) and the reverse primer (P501) each containing a unique index sequence were used (see Table S1). The PCR product was purified with 2% agarose gel and extracted using a gel extraction kit (IBI Scientific). The extracted DNA was eluted in 25 μL Milli-Q water and the concentration was quantified using a NanoDrop spectrophotometer to be 9 ng/ μL , and the sequencing was performed at McMaster University.

Activity assays. For cleavage activity assays, the DNazyme complex were prepared by annealing the FAM-labeled substrate (10 μM) and enzyme (30 μM) in buffer A. Other pH and salt concentrations were also tested. Assays were performed with a final concentration of 0.4 μM of the FAM-labeled substrate and 1.2 μM of the enzyme. A final of 0.05-200 μM Ag^+ was added to initiate the cleavage reaction. The products were separated on a denaturing PAGE gel and analyzed using a Bio-Rad Chemi-Doc MP imaging system. For determining the rate of cleavage, the gel

band intensities were quantified and the data obtained were fitted according to the first-order rate equation $Y_t = Y_o + a(1 - e^{-kx})$, where Y_t and Y_o are the cleavage fractions at a given reaction time t and time zero, respectively, and k is the rate constant.

Fluorescence-based Ag⁺ sensing. Sensor signaling kinetics were measured in 96-well plates using a microplate reader (SpectraMax M3). The sensing complex was formed by annealing 5'-FAM-Sub (10 μM) and the quencher-labeled enzyme (Ag10c-Q, 20 μM) in buffer (50 mM MOPS, pH 7.0 with 25 mM NaNO₃). Finally, 0.5 μL of the above annealed sensor was diluted with 97.5 μL buffer (50 mM MOPS pH 7.5, 200 mM NaNO₃) in the plate. A 2 μL amount of target ions was added to initiate the cleavage reaction. Samples were continuously monitored for at least 30 min with 20 sec intervals.

Results and Discussion

In vitro selection using Ag⁺. In vitro selection refers to the isolation of a subset of DNA sequences with a desired function from a large library.¹³ Our goal here was to obtain RNA-cleaving DNazymes that work specifically with Ag⁺. The scheme of selection is shown in Figure 1A. Our DNA library contains 50 random nucleotides (see Figure 1B for the library sequence), and a single RNA linkage (rA, denotes for ribo-adenine). Since RNA is much more susceptible to cleavage,³⁸ this is an artificially introduced cleavage site. The initial library contained ~10¹³ random DNA sequences. The role of metal ions in RNA cleavage has been extensively studied,^{39,40} and we hoped that certain DNA sequences can utilize Ag⁺ for this reaction. If this hypothesis is true, a fraction of the library (originally length = 119 nucleotide (nt)) might be cleaved at this RNA junction by Ag⁺ and thus became shorter by 28 nt. We harvested the cleaved fragment (91 nt) using denaturing

gel electrophoresis, and amplified it by two rounds of PCR to re-generate the full-length library for the next round of selection. PCR1 brings the library back to the original length, and PCR2 introduces the FAM fluorophore and rA.

Throughout the selection, the Ag^+ concentration was maintained at $10 \mu\text{M}$ with 1 h incubation time. The FAM label allowed us to quantify the cleavage yield at each round, and a gradual increase was observed (Figure 1C). However, this increase was quite slow. At round 6, only ~8% of the library was cleaved. This indicates that Ag^+ -dependent sequences did not dominate the library, and non-specific cleavage was competing. The gradually increased cleavage however still suggested a small population that might depend on Ag^+ . To identify this population, instead of the conventional cloning method, we resorted to deep sequencing at round 6; a total of 54,961 sequences were obtained.

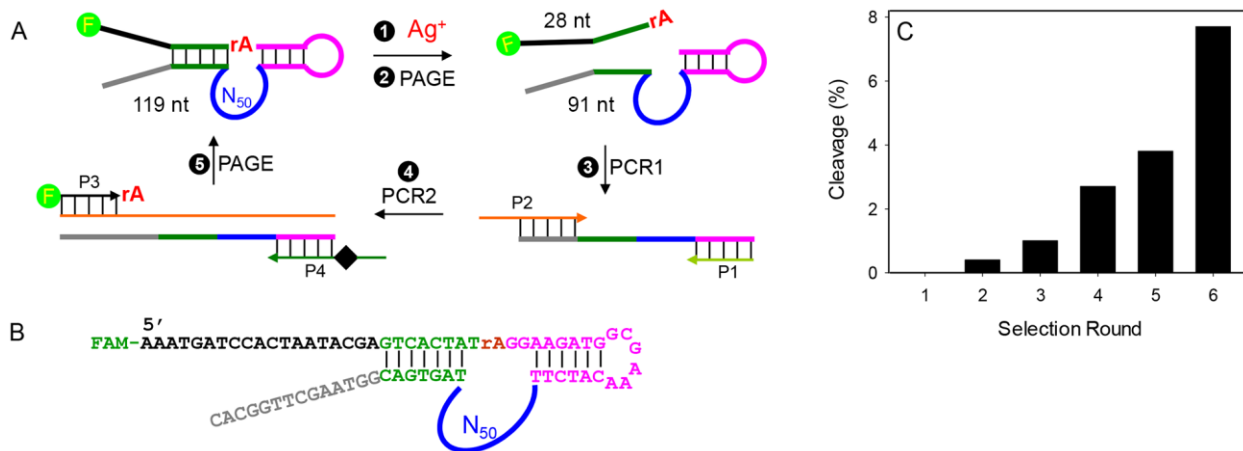


Figure 1. (A) The schematic representation of our in vitro selection with five steps. Ag^+ is used to induce cleavage. Two PCR steps are used to convert the cleaved sequence back to the original full length. The P4 primer has a polymer spacer (denoted by the black diamond) to stop the PCR extension, yielding two strands of unequal lengths. The shorter strand is harvested in step 5 for the next round of selection. (B) The sequence of the library for our in vitro selection with 50 random

nucleotides (N_{50}). The cleavage site is at the rAG junction. (C) Progress of our selection. At each round, $10\ \mu\text{M}$ Ag^+ with 1 h incubation was made in buffer A (50 mM MES, pH 6.0, 25 mM NaNO_3).

Sequence Analysis. Upon aligning the sequences, 874 families were obtained. The most populated first 200 families, accounting for 88.8% of all the sequences, were examined for their secondary structures using Mfold.⁴¹ Interestingly, a few families accounting to 1.5% of the analyzed sequences belong to the Ce13d DNAzyme or its variants, which was previously selected in our lab.^{24, 42} About 91% of the analyzed sequences contained a motif of TTCTCACA, which is a signature of another DNAzyme discovered in our lab, named EtNa.³⁰ EtNa is activated by Na^+ alone and accelerated by ethanol, and this may explain the large population of Ag^+ -independent sequences. Only 7.5 % of the analyzed sequences appeared novel, from which we engineered nineteen different trans-cleaving DNAzymes (Figure 2A). See Figure S1 for an example of converting the cis-cleaving Ag10 DNAzyme to its trans-cleaving form. The full-length trans-cleaving Ag10 DNAzyme is shown in Figure 3A. The enzyme strand binds the substrate using the two duplex regions, and the middle part is the catalytic core. In Figure 2A, the postulated catalytic cores are in boldface, and the rest of the sequences are the substrate binding arms (see table S1 for complete DNA sequences).

Each sequence in Figure 2A was individually tested by hybridizing with the FAM-labeled substrate in $10\ \mu\text{M}$ Ag^+ (Figure 2B). Significant cleavage after 1 h was observed only for two sequences (Ag9 and Ag10). Ag10 (marked in red) produced the highest cleavage and was studied further.

Enzyme	Sequence	Copy NO.
Ag1	-CGCCATCTT----- AACGCGCACGGCGGAACCCAC -----TAGTGACTC-	50
Ag2	-CGCC----- GGGATT -----TAGTGACTC-	25
Ag3	-CGCCATCTT----- GGGGGGCGGAAGGGCTGCGC -----TAGTGACTC-	82
Ag4	-CGCCAT----- GCGGAACCCACCTACACGGATGGC -----TAGTGACTC-	55
Ag5	-CGCCAT----- GGAACACACCCGGGG -----TAGTGACTC-	50
Ag6	-CGC----- GGTGG -----AGTGACTC-	47
Ag7	-CGCCATC-- CATAGCAGAGCGTCTAGAGATGTAAGTAAATCTTTTCTCAGCGAGACGAAA TAGTGACTC-	141
Ag8	-CGCCATCTT----- GGCGGACTGGGTGGCTGTGG -----TAGTGACTC-	92
Ag9	-CGCCATCTT TAGGCCTTAAACCCGTTGTAGGATTTGTAAGTCATTACTCTGAAGACGT -ATAGTGACTC-	438
Ag10	-CGCCATCTT TAGGTGATTTCCACGATAGAGAACTATTATGCGGAAACAGGGCAGCGT -ATAGTGACTC-	52
Ag11	-CGCCATCTT----- GTCCG -----GTGACTC-	30
Ag12	-CGCCATCTT----- GTCAACGACCGGGCCGGAAC -----TAGTGACTC-	27
Ag13	-CGCCATCTT----- GAGCATGAAGGCTCCATAAGTCGCGGG -----ATAGTGACTC-	26
Ag14	-CGCCATCTT TTAGAACTTAAATTCACGTAGCGCAAGGGGTGATATGAGGCGACCGTGT ATAGTGACTC-	24
Ag15	-CGCCATC----- GCGGTTAATTGAGTCGCACCGAC -----TAGTGACTC-	23
Ag16	-CGC----- ACCGAC -----TAGTGACTC-	20
Ag17	-CGCCATCTT----- GCACGGGGCGACATGTGGAT -----TAGTGACTC-	21
Ag18	-CGCCATCTT----- TGGCGTCACAGGATCGCGGT -----TAGTGACTC-	23
Ag19	-CGCCAT----- CGCGGAGATGTGTAGGCCGGGATT -----TAGTGACTC-	25

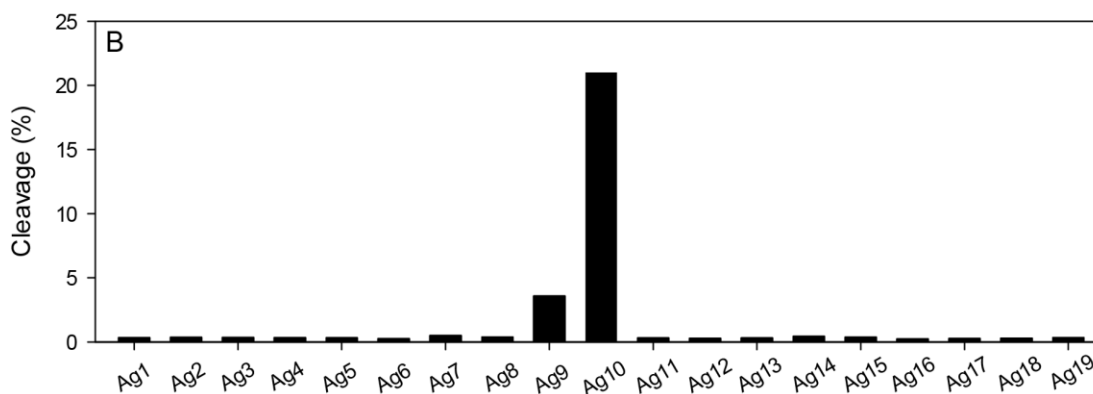


Figure 2. (A) The sequences of the 19 potential Ag⁺-dependent trans-cleaving DNAzymes from 5' to 3' with the hypothetical catalytic loop regions in bold. The catalytic loops are connected to the substrate binding arms. The copy number of each sequence from the sequencing results is also shown. The Ag10 sequence is in red. (B) Cleavage yield of the above sequences in buffer A with 10 μM Ag⁺ for 1 h.

Based on the secondary structure of Ag10 (Figure 3A), we truncated the nucleotides in black, which appear to be redundant. This truncated DNAzyme is named Ag10c (Figure 3B), which retained a similar activity as the original Ag10 DNAzyme (Figure 3C). Ag10c has a hairpin, and two long unpaired bulges connecting this hairpin to the two substrate binding arms. Such a structure is typical of RNA-cleaving DNAzymes,^{19, 24, 27, 30} and the hairpins usually play only a structural role. Metal binding is likely to take place in the large loop formed by the two unpaired bulges.

Since Ag⁺ is known to stabilize cytosine-cytosine mismatches,³¹ and this might be a way for Ag⁺ to exert an allosteric effect in promoting DNAzyme activity,^{35, 43} From this secondary structure, however, we cannot identify potential C-Ag⁺-C base pairs that can stabilize a stem-loop structure.⁴³ There are only three cytosine nucleotides on one side of the catalytic loop, and two more in the hairpin loop. Therefore, the role of Ag⁺ is likely to go beyond stabilization of simple DNAzyme secondary structures. We believe Ag⁺ might directly participate in catalysis, and biochemical characterization of Ag10c to support this hypothesis will be a subject of future studies. Since Ag10c is shorter than Ag10, it was used from this point on.

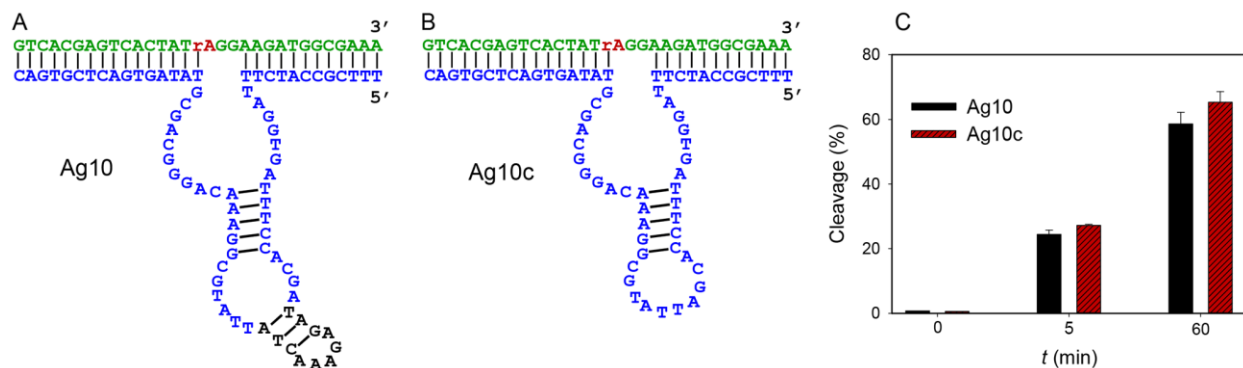


Figure 3. The secondary structures of (A) the Ag10 DNAzyme and (B) its truncated form Ag10c.

The substrate strand is in green and the enzymes in blue/black. (C) The cleavage yields of the two DNazymes with 10 μM Ag^+ at a few time points (buffer: 50 mM MOPS, pH 7.0, 25 mM NaNO_3).

Optimization of cleavage conditions. To identify an optimal condition for Ag^+ detection, we performed preliminary characterizations on Ag10c. We first studied the effect of pH (Figure 4A). The cleavage yields at two time points (5 and 60 min) were measured, and higher pH produced higher cleavage yields up to pH 8. Therefore, high pH is more favorable for the reaction, which might be related to the deprotonation of the 2'-OH of the RNA base, making it a better nucleophile.⁴⁴ The solubility limit of Ag^+ is about 1 mM at pH 9.⁴⁵ Therefore, we were far below this limit in the above experiments, and Ag^+ precipitation was not a concern here.

Next, we tested various concentrations of Ag^+ at pH 7.0 in 25 mM NaNO_3 by measuring the cleavage yield at 5 min. The yield was low below 1 μM Ag^+ , and it then rapidly increased (Figure 4B). The most optimal concentration was 10 μM Ag^+ . At even higher Ag^+ concentrations, inhibition was observed, which might be attributable to non-specific Ag^+ binding to DNA bases, inducing denaturation or misfolding of the DNzyme.

Under an optimal condition of pH 7.5 with 200 mM NaNO_3 and 10 μM Ag^+ , we measured the cleavage kinetics (Figure 4C). The kinetic profile was fitted to a first-order reaction with a rate constant of 0.41 min^{-1} . This is a very fast rate considering Ag^+ is a monovalent metal ion and no divalent metals were added. For comparison, the recently reported Na^+ -specific DNzyme has a rate of 0.11 min^{-1} with 400 mM Na^+ .¹⁴ This fast cleavage rate also suggests that Ag^+ might directly participate in catalysis. So far, no DNazymes with Na^+ alone can achieve such a high rate.^{26, 27, 30}

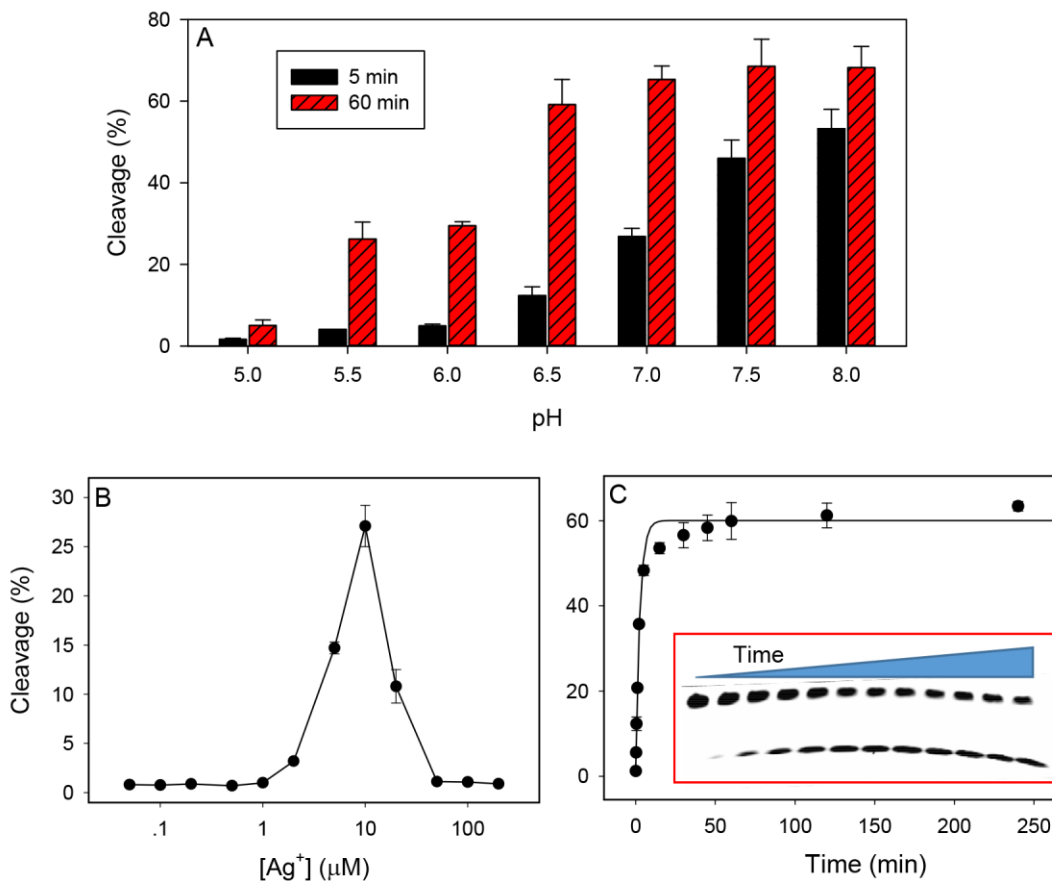


Figure 4. The cleavage yield of the Ag10c DNzyme at (A) different pH with 25 mM NaNO₃, (B) pH 7.0, 50 mM MOPS and 25 mM NaNO₃ at various Ag⁺ concentrations in 5 min. (C) Kinetics of Ag10c cleavage with 10 μM Ag⁺ at pH 7.5 with 200 mM NaNO₃, yielding a rate of 0.41 min⁻¹. Inset: a gel image at different time points (0, 0.16, 0.5, 1, 2, 5, 15, 30, 45, 60, 120 and 240 min). The upper bands are the original substrate and the lower bands are the cleavage product.

Chloride inhibition proving Ag⁺ requirement. As this is the first case of DNzyme catalysis using a monovalent transition metal ion, we performed the following experiment to confirm its Ag⁺ requirement. The cleavage yield of Ag10c was measured in the presence of increasing

concentrations of NaNO₃ or NaCl (Figure 5A). With NaNO₃, the cleavage reached a similar value for all the conditions (red bars), while a strong inhibition effect of NaCl was observed when the Cl⁻ was greater than 50 mM (black bars). The cleavage went to the background level with more than 100 mM NaCl. The solubility product (k_{sp}) of AgCl is 1.8×10^{-10} . Therefore, with 100 mM Cl⁻, the free Ag⁺ concentration is only ~18 nM. As will be seen later, the DNAzyme cannot detect Ag⁺ beyond this level. Since NaNO₃ did not decrease the cleavage yield, the inhibition by NaCl cannot be attributed to the change in ionic strength. Taken together, the inhibition effect of NaCl is attributable to complex formation with Ag⁺ or forming AgCl precipitation. This experiment provides a strong evidence that Ag⁺ is critical for the activity of the DNAzyme.

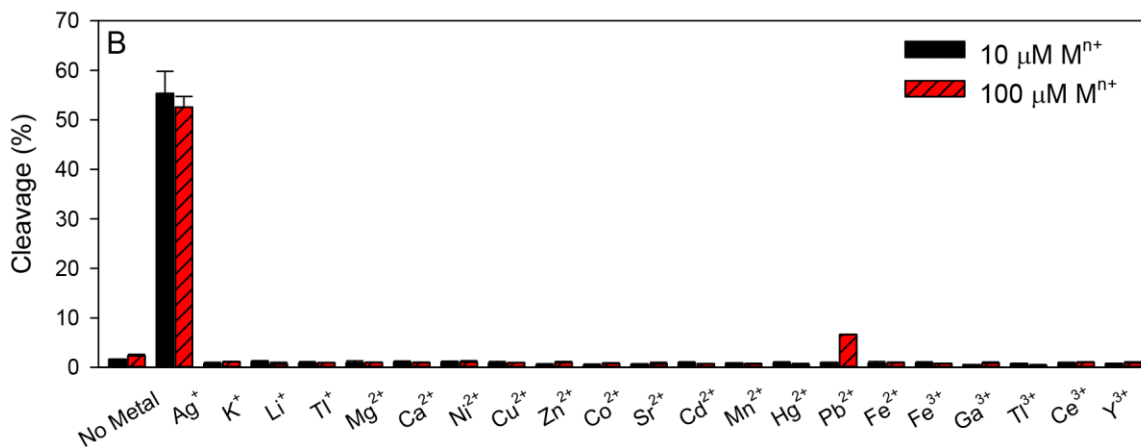
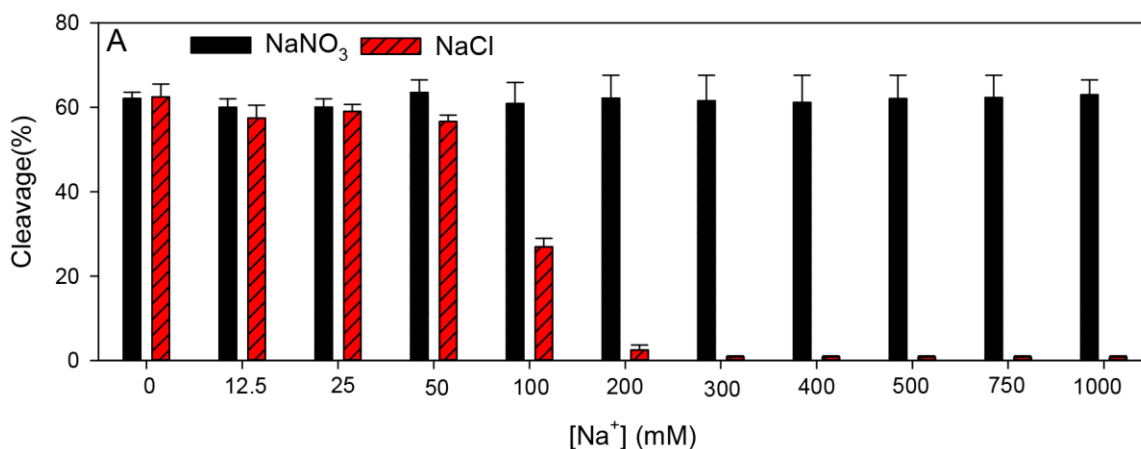


Figure 5. (A) The cleavage yield of Ag10c in presence of 10 μM Ag^+ and various concentrations of NaCl or NaNO_3 . (B) Cleavage yield with Ag^+ as compared to 10 μM and 100 μM of 20 other metals. All the reactions were performed in 50 mM MOPS, pH 7.0 for 1 h. While 100 μM Pb^{2+} showed a modest cleavage, its rate is >3000-fold slower compared to the same concentration of Ag^+ .

Ag10c is highly specific for Ag^+ . Our in vitro selection was carried out with Ag^+ and no negative selections were performed. For Ag^+ sensing, metal specificity is also very important. We next tested Ag10c in the presence of 10 μM and 100 μM of 20 different metal ions (Figure 5B). Indeed, Ag10c is highly specific for Ag^+ and it has negligible or no activity in the presence of any other metal. Only 100 μM Pb^{2+} produced a very moderate cleavage of ~8% after 1 h. The interference by Pb^{2+} is commonly seen in the DNAzyme field,^{24, 46} possibly due to the close to neutral $\text{p}K_a$ value of the Pb^{2+} bound water,⁴⁷ making it ideal for activating the 2'-OH nucleophile. Even for Pb^{2+} , the rate of cleavage ($\sim 0.0013 \text{ min}^{-1}$ with 100 μM Pb^{2+}) under the same metal concentration is still >3000-fold slower compared to that for Ag^+ (0.41 min^{-1} with 10 μM Ag^+). For the other metals, the selectivity of Ag10c for Ag^+ is even higher, making it an excellent probe for Ag^+ sensing.

A silver biosensor. From the studies above, it is clear that Ag10c is highly specific for Ag^+ with fast catalytic rate, allowing building a biosensor for Ag^+ . Among the various signaling strategies, we herein employed a catalytic beacon method for its high sensitivity.^{6, 46} We labeled the 3'-end of the enzyme strand with a Black Hole Quencher (named Ag10c-Q in Table S1), which upon hybridization, quenches the fluorescence of the FAM fluorophore labeled on the 5'-end of the

substrate (5'-FAM-Sub). In the presence of Ag^+ , cleavage of the substrate rescues the fluorescence after releasing the cleaved fragment (Figure 6A). The structure of the sensor DNzyme complex is shown in Figure S2.

We executed this experiment with increasing concentration of Ag^+ by monitoring the signaling kinetics at pH 7.5, 50 mM MOPS, 200 mM NaNO_3 (Figure 6B). In the absence of Ag^+ , the background was quite stable, indicating a stable DNzyme complex. The rate of fluorescence enhancement rapidly increased with higher Ag^+ concentration. We quantified the initial rates in Figure 6C, and the dynamic range reached ~ 400 nM Ag^+ . The low Ag^+ concentration region is shown in the inset of Figure 6C, and we calculated a limit of detection (LOD) of 24.9 nM Ag^+ based on $3\sigma/\text{slope}$ (σ is the standard deviation of the background signal). This is 37-fold lower than the maximum permissible contamination level of silver in water i.e. 0.1 mg/L or 930 nM defined by the World Health Organization.

To test for selectivity, the sensor was then challenged with various monovalent, divalent and trivalent cations. The signal remained at the background level with most ions, while a few caused fluorescence quenching. The only one (except Ag^+) with fluorescence increase was Hg^{2+} , both a 1 μM and at 100 μM concentrations. Since the gel-based assay with similar concentrations of Hg^{2+} did not produce any cleavage (Figure 5B), we speculated that the fluorescence increase was from Hg^{2+} -induced DNA misfolding. Hg^{2+} has strong affinity with DNA pyrimidine bases, which may fold the FAM label away from the quencher, thus enhancing the fluorescence. If this hypothesis is true, such a rise in fluorescence should be reversible if the Hg^{2+} ions are made unavailable. To test it, we initiated the rise in fluorescence with 1 μM Hg^{2+} or 400 nM Ag^+ . Upon signal stabilization, 10 μM NaI was added to both reactions (Figure 6E). Indeed, in the Hg^{2+} reaction, the signal went back to the background level due to HgI_2 formation, while no change was

seen in the Ag^+ reaction upon formation of AgI , proving that the sensor was irreversibly cleaved by silver ions. It might be possible to eliminate the signal from Hg^{2+} by using other designs, such as gold nanoparticle based colorimetric sensors,⁴⁸ or using more stably folded DNAzyme secondary structures.⁴⁹ While Pb^{2+} showed a slight cleavage in gel-based assay, its rate is >3000-fold slower than Ag^+ , and Pb^{2+} is a strong fluorescence quencher at high concentrations. These factors may explain the lack of Pb^{2+} response in this rate-based signaling method.

Further, we wanted to study if this sensor works in real world water samples. For this, our sensor was tested in Lake Huron water with 50 mM MOPS buffer (pH 7.5, 90% of lake water in the final reaction, Figure 6F). The response was quite similar to that obtained in clean buffers, and a LOD of 21.8 nM was calculated (Figure S3). Therefore, the lake water matrix did not interfere with the detection. The Great Lake's water often contains below 1 mM Cl^- ,⁵⁰ and therefore it is understandable that the sensitivity of our sensor was not affect.

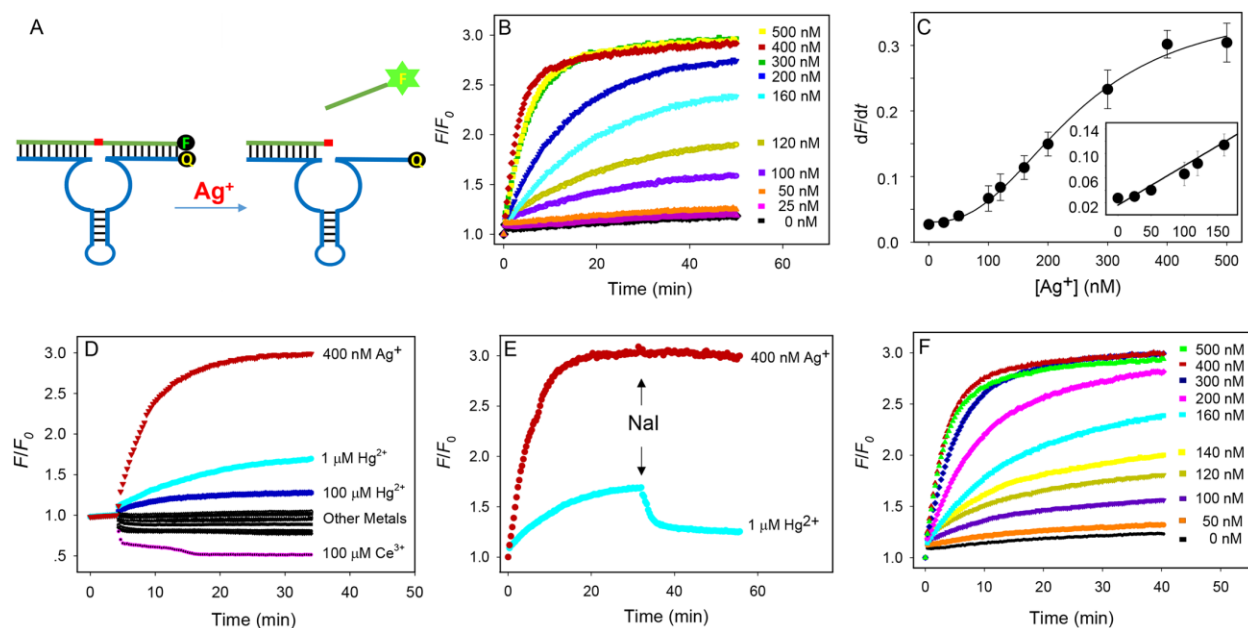


Figure 6. (A) Schematic representation of the Ag^+ DNAzyme beacon design. (B) Sensor signaling kinetics at various concentrations of Ag^+ . (C) Quantification of Ag^+ based on the initial rate of

fluorescence enhancement. Inset: the low Ag^+ concentration region fitted with a linear response. Sensor signaling kinetics with (D) various metal ions: 1 and 100 mM K^+ , Li^+ , Rb^+ , Na^+ , Cs^+ ; 1 and 10 mM Ca^{2+} , Mg^{2+} , 1 and 100 μM Mn^{2+} , Fe^{2+} , Cu^{2+} , Zn^{2+} , Ni^{2+} , Co^{2+} , Cd^{2+} , Pb^{2+} , Sr^{2+} , Ce^{3+} and Fe^{3+} . (E) Sensor response to 400 nM Ag^+ and 1 μM Hg^{2+} where the black arrows indicate the time of addition of 10 μM NaI. The fluorescence dropping in the Hg^{2+} reaction indicates its signaling was not due to cleavage. All the reactions were performed in 50 mM MOPS, pH 7.5 with 200 mM NaNO_3 . The final sensor concentration was 50 nM. (F) Detecting spiked Ag^+ in Lake Huron water.

Conclusions

In conclusion, we reported the first Ag^+ - specific RNA-cleaving DNAzyme, which was evolved in course of an in vitro selection effort using silver as the intended metal cofactor. This enzyme named Ag10c, shows high selectivity for silver over other metal ions and a fast catalytic rate of 0.41 min^{-1} at pH 7.5 and 200 mM NaNO_3 with just 10 μM Ag^+ . This study highlights the possibility of using monovalent transition metal ions as a cofactor for DNAzyme catalysis. We have also demonstrated the use of this DNAzyme for selectively sensing low concentrations of Ag^+ ions, with the LOD of the sensor being 24.9 nM, which is far below the permissible limit of silver in water. Taken together, this enzyme is not only a useful analytical probe for silver, but also gives a platform to study the role of monovalent ions in DNAzyme catalysis.

Supporting Information Available:

DNA sequences, DNAzyme secondary structures, and detection in Lake Huron water. This information is available free of charge via the Internet at <http://pubs.acs.org/>.

Acknowledgement

This work is supported by the Natural Sciences and Engineering Research Council of Canada (NSERC) Strategic Project Grant: STPGP-447472-2013.

References

- (1) Drake, P. L.; Hazelwood, K. J. *Ann. Occup. Hyg.* **2005**, *49*, 575-585.
- (2) Ratte, H. T. *Environ. Toxicol. Chem.* **1999**, *18*, 89-108.
- (3) Coskun, A.; Akkaya, E. U. *J. Am. Chem. Soc.* **2005**, *127*, 10464-10465.
- (4) Chatterjee, A.; Santra, M.; Won, N.; Kim, S.; Kim, J. K.; Bin Kim, S.; Ahn, K. H. *J. Am. Chem. Soc.* **2009**, *131*, 2040-2041.
- (5) Zhang, X.-B.; Kong, R.-M.; Lu, Y. *Annu. Rev. Anal. Chem.* **2011**, *4*, 105-128.
- (6) Liu, J.; Cao, Z.; Lu, Y. *Chem. Rev.* **2009**, *109*, 1948-1998.
- (7) Schlosser, K.; Li, Y. F. *Chem. Biol.* **2009**, *16*, 311-322.
- (8) Song, S. P.; Qin, Y.; He, Y.; Huang, Q.; Fan, C. H.; Chen, H. Y. *Chem. Soc. Rev.* **2010**, *39*, 4234-4243.
- (9) Wang, H.; Yang, R. H.; Yang, L.; Tan, W. H. *ACS Nano* **2009**, *3*, 2451-2460.
- (10) Katz, E.; Willner, I. *Angew. Chem., Int. Ed.* **2004**, *43*, 6042-6108.
- (11) Lu, Y. *Inorg. Chem.* **2006**, *45*, 9930-9940.
- (12) Liu, J. *Can. J. Chem.* **2015**, *93*, 273-278.
- (13) Joyce, G. F. *Ann. Rev. Biochem.* **2004**, *73*, 791-836.
- (14) Lu, Y. *Chem. Eur. J.* **2002**, *8*, 4588-4596.
- (15) Breaker, R. R.; Joyce, G. F. *Chem. Biol.* **1994**, *1*, 223-229.

- (16) Li, J.; Zheng, W.; Kwon, A. H.; Lu, Y. *Nucleic Acids Res.* **2000**, *28*, 481-488.
- (17) Carmi, N.; Balkhi, H. R.; Breaker, R. R. *Proc. Natl. Acad. Sci. U.S.A.* **1998**, *95*, 2233-2237.
- (18) Cuenoud, B.; Szostak, J. W. *Nature* **1995**, *375*, 611-614.
- (19) Liu, J.; Brown, A. K.; Meng, X.; Cropek, D. M.; Istok, J. D.; Watson, D. B.; Lu, Y. *Proc. Natl. Acad. Sci. U.S.A.* **2007**, *104*, 2056-2061.
- (20) Huang, P.-J. J.; Liu, J. *Nucleic Acids Res.* **2015**, *43*, 6125-6133.
- (21) Hollenstein, M.; Hipolito, C.; Lam, C.; Dietrich, D.; Perrin, D. M. *Angew. Chem., Int. Ed.* **2008**, *47*, 4346 - 4350.
- (22) Huang, P.-J. J.; Vazin, M.; Matuszek, Z.; Liu, J. *Nucleic Acids Res.* **2015**, *43*, 461-469.
- (23) Huang, P.-J. J.; Vazin, M.; Liu, J. *Anal. Chem.* **2014**, *86*, 9993-9999.
- (24) Huang, P.-J. J.; Lin, J.; Cao, J.; Vazin, M.; Liu, J. *Anal. Chem.* **2014**, *86*, 1816-1821.
- (25) Roth, A.; Breaker, R. R. *Proc. Natl. Acad. Sci. U.S.A.* **1998**, *95*, 6027-6031.
- (26) Geyer, C. R.; Sen, D. *Chem. Biol.* **1997**, *4*, 579-593.
- (27) Torabi, S.-F.; Wu, P.; McGhee, C. E.; Chen, L.; Hwang, K.; Zheng, N.; Cheng, J.; Lu, Y. *Proc. Natl. Acad. Sci. U.S.A.* **2015**, *112*, 5903-5908.
- (28) Zhou, W.; Zhang, Y.; Huang, P.-J. J.; Ding, J.; Liu, J. *Nucleic Acids Res.* **2016**, *44*, 354-363.
- (29) Torabi, S.-F.; Lu, Y. *J. Mol. Evol.* **2015**, *81*, 225-234.
- (30) Zhou, W.; Saran, R.; Chen, Q.; Ding, J.; Liu, J. *ChemBioChem* **2016**, *17*, 159-163.
- (31) Ono, A.; Cao, S.; Togashi, H.; Tashiro, M.; Fujimoto, T.; Machinami, T.; Oda, S.; Miyake, Y.; Okamoto, I.; Tanaka, Y. *Chem. Commun.* **2008**, 4825-4827.
- (32) Urata, H.; Yamaguchi, E.; Nakamura, Y.; Wada, S.-I. *Chem. Commun.* **2011**, *47*, 941-943.
- (33) Freeman, R.; Finder, T.; Willner, I. *Angew. Chem., Int. Ed.* **2009**, *48*, 7818-7821.
- (34) Wen, Y. Q.; Xing, F. F.; He, S. J.; Song, S. P.; Wang, L. H.; Long, Y. T.; Li, D.; Fan, C. H. *Chem. Commun.* **2010**, *46*, 2596-2598.

- (35) Li, T.; Shi, L.; Wang, E.; Dong, S. *Chem. Eur. J.* **2009**, *15*, 3347-3350.
- (36) Su, Y.-T.; Lan, G.-Y.; Chen, W.-Y.; Chang, H.-T. *Anal. Chem.* **2010**, *82*, 8566-8572.
- (37) Richards, C. I.; Choi, S.; Hsiang, J.-C.; Antoku, Y.; Vosch, T.; Bongiorno, A.; Tzeng, Y.-L.; Dickson, R. M. *J. Am. Chem. Soc.* **2008**, *130*, 5038-5039.
- (38) Li, Y.; Breaker, R. R. *J. Am. Chem. Soc.* **1999**, *121*, 5364-5372.
- (39) Ward, W. L.; Plakos, K.; DeRose, V. J. *Chem. Rev.* **2014**, *114*, 4318-4342.
- (40) Sigel, R. K. O.; Pyle, A. M. *Chem. Rev.* **2007**, *107*, 97-113.
- (41) Zuker, M. *Nucleic Acids Res.* **2003**, *31*, 3406-3415.
- (42) Vazin, M.; Huang, P.-J. J.; Matuszek, Z.; Liu, J. *Biochemistry* **2015**, *54*, 6132-6138.
- (43) Liu, J.; Lu, Y. *Angew. Chem., Int. Ed.* **2007**, *46*, 7587-7590.
- (44) Dahm, S. C.; Derrick, W. B.; Uhlenbeck, O. C. *Biochemistry* **1993**, *32*, 13040-13045.
- (45) Sauls, F. C. *J. Chem. Edu.* **2013**, *90*, 1212-1214.
- (46) Li, J.; Lu, Y. *J. Am. Chem. Soc.* **2000**, *122*, 10466-10467.
- (47) Burgess, J. *Metal ions in solution*; Ellis Horwood Ltd. : Chichester, **1978**.
- (48) Liu, J. W.; Lu, Y. *J. Am. Chem. Soc.* **2003**, *125*, 6642-6643.
- (49) Li, H.; Zhang, Q.; Cai, Y.; Kong, D.-M.; Shen, H.-X. *Biosens. Bioelectron.* **2012**, *34*, 159-164.
- (50) Dove, A. *Aquat. Ecosyst. Health.* **2009**, *12*, 281-295.